Pergamon

Int. J. Solids Structures Vol. 34, No. 15, pp. 1825–1847, 1997

0020-7683/97 $17.00 + .00

PII : S0020-7683(96)00125-4

FOLDABLE BAR STRUCTURES

Z. YOU and S. PELLEGRINO
Department of Engineering, Cambridge University, Trumpington Street,
Cambridge CB2 1PZ, UK

(*Received* 5 *March* 1996; *in revised form* 19 *June* 1996)

Abstract—A new, general type of two-dimensional foldable structures is presented, which extends and generalises the standard trellis-type foldable structure consisting of two sets of parallel *straight rods* connected by hinges. It is shown that any structure consisting of rigid, *multi-angulated rods*, i.e., straight rods with kinks at the hinge positions, can be folded if the rods form a tessellation of parallelograms. This discovery is exploited to investigate the structural layouts of flat and curved structures which can be folded along their perimeter. © 1997 Elsevier Science Ltd.

1. INTRODUCTION

A simple, two-dimensional foldable structure can be made from two sets of parallel, straight rods connected by pivots, or *scissor hinges*, at all intersection points. A scissor hinge is a revolute joint whose axis is perpendicular to the plane of the structure. Both structures shown in Fig. 1 are of this type, and both can be folded by freely deforming their cells in shear until the two sets of rods become approximately parallel, for $\theta \cong 0^\circ$ or $\theta \cong 180^\circ$. During folding, each set of collinear pivots remains collinear, and all pivots become collinear—in theory, at least—in the fully-folded configuration. This is the principle behind many commonly used foldable structures, e.g. garden trellises, wine racks, awnings, etc. The same concept has already been used for more exotic applications, such as movable theatre structures (Pinero, 1961, Escrig, 1993), but it affords only limited freedom to engineers designing structures whose shape, boundaries, etc. are already specified. Hence, numerous efforts have been made to find more general solutions.

Broadly speaking, there are two different ways of extending this simple, intuitive concept to more general shapes. One option is to look for a repeating building block with an internal degree of freedom which allows folding; another option is to design a complete structure, whose shape is determined mainly by its particular application, and then to modify its geometry, member properties and layout, connections, etc. until the structure can be folded and deployed without damage, albeit with some elastic deformation of its members.

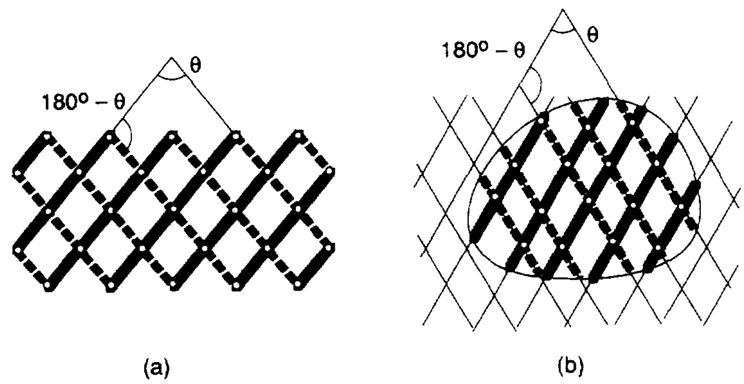

Fig. 1. Trellis-type foldable structures formed by two sets of straight, parallel rods.

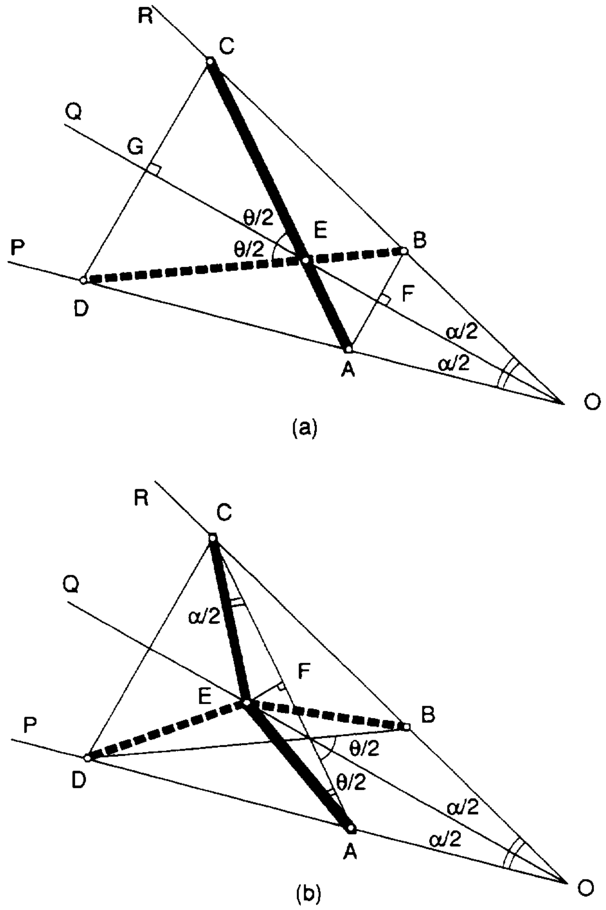

Fig. 2. (a) Ordinary pantographic element consisting of straight rods. (b) Symmetric angulated element with a constant angle of embrace and $\overline{AE} = \overline{BE} = \overline{CE} = \overline{DE}$.

The advantage of the first, modular approach is that, once a suitable building block has been found, then a whole class of foldable structures may become available simply by changing the number and size of the blocks. Two- and three-dimensional assemblies of pairs of straight bars connected by scissor hinges, which form single-degree-of-freedom mechanisms (Clarke, 1984, Escrig, 1985), have been used as building blocks for many complex structural mechanisms (Zanardo, 1986, Kwan and Pellegrino, 1991). However, it is not generally true that a structure consisting of foldable modules is always foldable: it is also required that the interfaces between modules deform in a compatible fashion, and in some cases there may also be one or more global conditions that need to be satisfied (Pellegrino and You, 1993, You and Pellegrino, 1994).

A recent development, of crucial importance to this paper, was the invention of the simple *angulated element* (Hoberman, 1990), consisting of a pair of identical angulated rods connected together by a scissor hinge, see Figs 2 and 3. In analogy with elements made from straight rods, which—under certain conditions—fold while maintaining the end pivots on parallel lines, angulated elements subtend a constant angle as their rods rotate. This property is exploited in Hoberman's foldable sculptures (Waters, 1992) and in Servadio's foldable polyhedra (1994). Among the more practical applications of simple angulated elements is the Iris Retractable Roof (Hoberman, 1991), a foldable dome with circular plan consisting of concentric rings connected by scissor hinges.

This approach to foldable bar structures has already produced many ingenious solutions, but real, large scale applications have yet to follow. A key disadvantage of this approach is that any solution is, in a sense, unique, i.e., valid only for a particular shape of structure and for a specific set of boundary conditions. Furthermore, the number of solutions currently known is quite small. For example, when designing the plan shape of

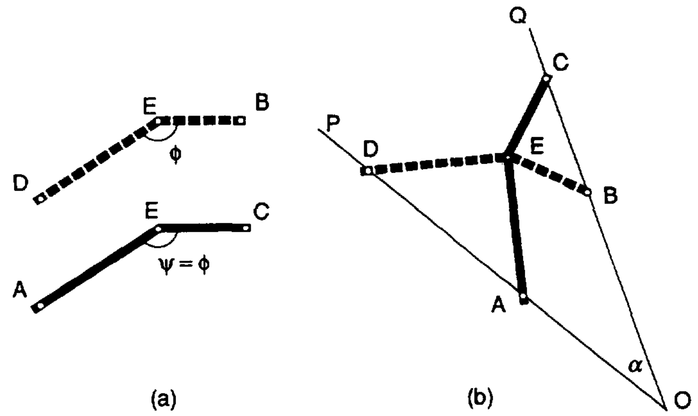

Fig. 3. General type of Hoberman's element, formed by *identical* angulated rods: $\overline{AE} = \overline{DE}$, $\overline{BE} = \overline{CE}$, $\psi = \varphi$. ADE and BCE are similar isosceles triangles.

the Iris Retractable Roof there are only three free parameters, which are the total number of rings, the number of angulated elements in each ring, and the length of the angulated rods. Everything else follows from geometric rules.

The second, global approach to the design of foldable bar structures has been pioneered by Pinero (1961) and Zeigler (1981, 1984, 1987, 1993) and has been further developed by Escrig *et al.* (1989) and Escrig and Valcarcel (1993). The idea is to design foldable structures by a two-stage process. First, the overall geometry of the structure is decided, such that all members are unstrained both in the required, fully deployed configuration and also in the folded configuration, usually a compact bundle where all bars are theoretically parallel. Second, a detailed structural analysis of the folding process is carried out, to check that any strains induced by the folding process are sufficiently small (Gantes *et al.*, 1991). Most foldable structures based on this approach consist of pairs of straight rods connected by off-centre scissor hinges. In general, the achievement of satisfactory behaviour during folding is at the expense of low deployed stiffness, and hence locking elements are usually incorporated in structures of this type. Although, in principle, any solution can be modified to suit the requirements of a particular application, even small changes will require some re-analysis.

We have recently discovered (You and Pellegrino, 1996) a new approach to foldable bar structures which combines the key advantages of the two approaches described above. This new approach makes use of a new, large family of foldable building blocks, which we call *generalised angulated elements*. These elements subtend a constant angle during folding, as Hoberman's simple angulated element, but afford much greater freedom than all other elements that have been used previously. We have also discovered that a series of contiguous angulated rods can be replaced with a single, *multi-angulated rod*, which is an extension of the straight rod with collinear pivots used in the simple foldable structures shown in Fig. 1, thus reducing significantly the number of component parts of a structure and the complexity of its joints. These two discoveries open up a range of new applications for large scale, foldable bar structures.

Although our discoveries are not restricted to a particular type of application, the examples that are presented in the paper are aimed towards foldable roof structures for stadia, swimming pools, etc. (Levy, 1995).

The layout of the paper is as follows. Section 2 briefly reviews the derivation of the simple angulated element. Section 3 introduces the new generalised angulated elements (GAE's), which consist of chains of any number of parallelograms, connected to adjacent elements either by two isosceles triangles, or by two similar triangles. The special properties of symmetric GAEs are discussed. Section 4 deals with assemblies of simple angulated elements that form circular, rotationally symmetric foldable structures. Starting from the solution originally proposed by Hoberman, consisting of separate angulated elements connected by scissor hinges, it is shown that a geometrically identical, but more efficient foldable structure can be made from multi-angulated elements. Section 5 deals with foldable structures of general shape, consisting of generalised angulated elements. Several configurations for foldable roof structures which can be folded along their perimeter, and have different shape, e.g. rectangular, elliptical, etc., are presented. Section 6 shows that three-dimensional variants of the solutions obtained in the paper can be obtained by projecting any of these layouts onto a three-dimensional surface. Double-layer foldable structures are also obtained in a similar way. Section 7 concludes the paper.

2. HOBERMAN'S ANGULATED ELEMENT

Figure 2(a) shows an ordinary pantographic element, made of a pair of *identical straight rods*, hinged together by a scissor hinge at E. The end connectors, A, B, C, and D define two straight lines OP and OR. The element is symmetric with respect to the line OQ. A relationship between α, the angle subtended by this element, and θ, the *deployment angle*, can be obtained by noting that

$$\overline{CG} - \overline{BF} = \overline{FG} \tan \alpha/2 \tag{1}$$

where

$$\overline{CG} = \overline{CE} \sin \theta/2 \tag{2}$$

$$\overline{BF} = \overline{BE} \sin \theta/2 = \overline{AE} \sin \theta/2 \tag{3}$$

and

$$\overline{FG} = \overline{AC} \cos \theta/2. \tag{4}$$

Substituting eqns (2)–(4) into eqn 1

$$(\overline{CE} - \overline{AE}) \sin \theta/2 = \overline{AC} \cos \theta/2 \tan \alpha/2 \tag{5}$$

or

$$\tan \alpha/2 = \frac{\overline{CE} - \overline{AE}}{\overline{AC}} \tan \theta/2. \tag{6}$$

It is obvious from eqn (6) that α varies with θ. Supposing that the positions of OP and OR are fixed, it can be concluded that it is impossible to mobilise the pantographic element ABCD, i.e., to vary the angle θ, if A, D and B, C are allowed to move only along the lines OP and OR (Zanardo, 1986).

This difficulty can be resolved (Hoberman, 1990, 1991) by using non-straight, "angulated" rods, and hence by moving the pivot E to the new, special position shown in Fig. 2(b). It can be readily shown that

$$\tan \alpha/2 = \frac{\overline{CF} - \overline{AF}}{\overline{AC}} \tan \theta/2 + 2\frac{\overline{EF}}{\overline{AC}}. \tag{7}$$

For $\overline{AF} = \overline{CF}$, i.e., F half way between A and C, the first term on the right-hand-side vanishes. Hence, α becomes a constant for all θs, and it is now possible to mobilise the pantographic element with A, D and B, C lying, respectively, on the lines OP and OR.

Therefore, deployment requires that the following two conditions be satisfied

$$\overline{AF} = \overline{CF} \quad \text{and} \quad \alpha = 2 \arctan \frac{\overline{EF}}{\overline{AF}}. \tag{8}$$

From eqn (8), it can be shown that

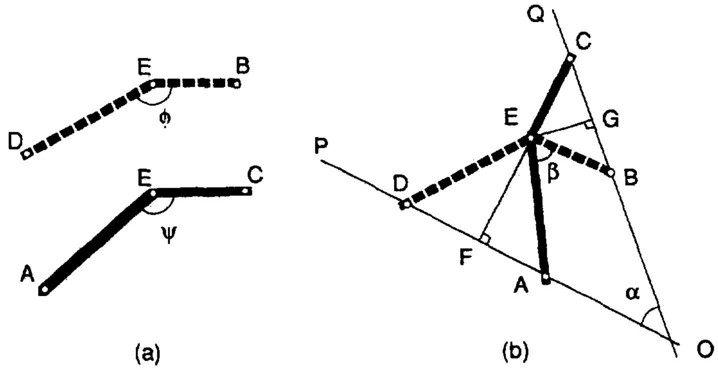

Fig. 4. Simplest Type I GAE, formed by angulated rods with equal semi-length but different kink angles $\overline{AE} = \overline{DE}$, $\overline{BE} = \overline{CE}$, $\psi \neq \varphi$. ADE and BCE are isosceles triangles.

$$\angle CAE = \angle ACE = \alpha/2 \tag{9}$$

$$\angle AEC = 180^\circ - \alpha \tag{10}$$

and hence the distance between an end hinge and the internal hinge is a constant

$$l = \sqrt{\overline{AF}^2 + \overline{EF}^2}. \tag{11}$$

Hoberman (1990, 1991) has shown that the above derivation can be extended to non-symmetric angulated elements, which are still made of *identical angulated rods*. Figure 3 shows the most general element considered by Hoberman. It satisfies the following conditions

$$\overline{AE} = \overline{DE}, \quad \overline{BE} = \overline{CE}, \quad \text{and} \quad \psi = \phi = 180^\circ - \alpha \tag{12}$$

and hence the angulated rods form two *isosceles triangles*. Note that $\overline{AE}$ is not necessarily equal to $\overline{BE}$.

3. GENERALISED ANGULATED ELEMENTS

A generalised angulated element (GAE) is a set of interconnected angulated rods that form *a chain of any number of parallelograms with either isosceles triangles* (Type I GAE) or *similar triangles* (Type II GAE) *at either end*. A generalised angulated element embraces a constant angle as the element is folded or expanded. Separate proofs of the angles of embrace of Type I and Type II GAEs are given next.

GAEs without any parallelograms are considered first, for simplicity, and it is shown that Hoberman's simple angulated element is a special case of both Type I and Type II GAEs.

3.1. *Type I GAE*

Before discussing the general Type I GAE, consider first the angulated element shown in Fig. 4, which has

$$\overline{AE} = \overline{DE}, \quad \overline{BE} = \overline{CE} \quad \text{and, in general,} \ \psi \neq \phi. \tag{13}$$

From Fig. 4, the sum of the internal angles in the quadrangle OGEF is 360° and, since $\angle OFE = \angle OGE = 90^\circ$, the angle α can be expressed as

$$\alpha = 180^\circ - (\angle AEF + \beta + \angle BEG). \tag{14}$$

Because $\triangle ADE$ and $\triangle BCE$ are isosceles triangles,

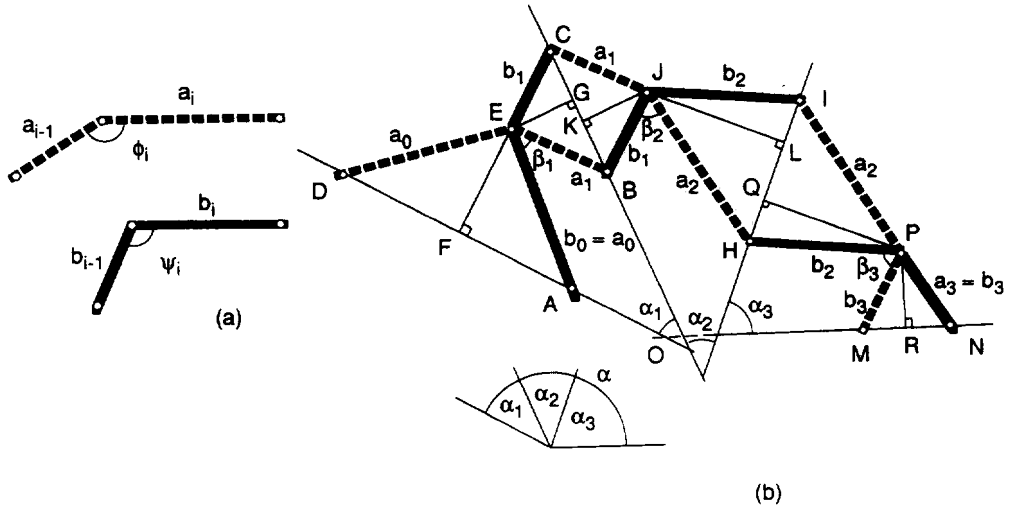

Fig. 5. General Type I GAE consisting of two isosceles triangles connected by two parallelograms.

$$\angle \mathrm{AEF} = \frac{\phi - \beta}{2} \quad \text{and} \quad \angle \mathrm{BEG} = \frac{\psi - \beta}{2}. \tag{15}$$

Hence, substituting eqn (15) into eqn (14)

$$\alpha = 180^\circ - \frac{\phi + \psi}{2} = \text{constant} \tag{16}$$

which shows that this element subtends a constant angle. Note that Hoberman's element is re-obtained, when $\phi = \psi$.

A most interesting special case is obtained when either $\phi = 180^\circ$, or $\psi = 180^\circ$, which implies that one rod is angulated, while the other rod is straight.

More general Type I GAEs are made from two or more angulated elements. Figure 5 shows an example with three elements, which satisfy the following conditions:

(i) each closed loop is a parallelogram, i.e.,

$$\overline{\mathrm{CE}} = \overline{\mathrm{BJ}} \quad \text{and} \quad \overline{\mathrm{EB}} = \overline{\mathrm{CJ}}, \quad \overline{\mathrm{HJ}} = \overline{\mathrm{IP}} \quad \text{and} \quad \overline{\mathrm{IJ}} = \overline{\mathrm{HP}}. \tag{17}$$

(ii) $\triangle$AED and $\triangle$NPM are isosceles triangles, i.e.,

$$\frac{\overline{\mathrm{DE}}}{\overline{\mathrm{AE}}} = \frac{\overline{\mathrm{MP}}}{\overline{\mathrm{NP}}} = 1. \tag{18}$$

Note that the structure shown in Fig. 5 can be regarded as being formed by "cutting" the element shown in Fig. 4 at the scissor hinge E and inserting parallelograms in between the triangles formed thus.

Next, it will be shown that the angle α embraced by this element has constant magnitude. From Fig. 5, it can be obtained that

$$\alpha = \angle \mathrm{DON} = \alpha_1 + \alpha_2 + \alpha_3 \tag{19}$$

where

$$\alpha_1 = 180^\circ - (\angle \mathrm{AEF} + \beta_1 + \angle \mathrm{BEG})$$

$$\alpha_2 = 180^\circ - (\angle \mathrm{BJK} + \beta_2 + \angle \mathrm{HJL})$$

$$\alpha_3 = 180^\circ - (\angle \mathrm{HPQ} + \beta_3 + \angle \mathrm{MPR}). \tag{20}$$

Condition (i) implies

$$\angle \mathrm{BEC} = \angle \mathrm{BJC} \quad \text{and} \quad \angle \mathrm{HJI} = \angle \mathrm{HPI} \tag{21}$$

and also

$$\angle \mathrm{BEG} + \angle \mathrm{BJK} = \angle \mathrm{BEC} \quad \text{and} \quad \angle \mathrm{HJL} + \angle \mathrm{HPQ} = \angle \mathrm{HJI}. \tag{22}$$

Substituting eqns (20), (21) and (22) into eqn (19) gives

$$\alpha = 3 \times 180^\circ - (\angle \mathrm{AEF} + \psi_1 + \psi_2 + \beta_3 + \angle \mathrm{MPR}). \tag{23}$$

From condition (ii), we know that

$$\angle \mathrm{AEF} = \frac{\angle \mathrm{AED}}{2} = \frac{\phi_1 - \beta_1}{2} \quad \text{and} \quad \angle \mathrm{MPR} = \frac{\angle \mathrm{MPN}}{2} = \frac{\psi_3 - \beta_3}{2}. \tag{24}$$

Note that eqn (21) can be rewritten as

$$\psi_1 - \beta_1 = \phi_2 - \beta_2 \quad \text{and} \quad \psi_2 - \beta_2 = \phi_3 - \beta_3 \tag{25}$$

and adding up these two equations gives

$$\psi_1 + \psi_2 - \beta_1 = \phi_2 + \phi_3 - \beta_3. \tag{26}$$

Adding $\phi_1 + \psi_3$ to both sides of eqn (26) and tidying up gives

$$\phi_1 - \beta_1 = \Sigma\phi - \Sigma\psi + \psi_3 - \beta_3 \tag{27}$$

where

$$\Sigma\phi = \phi_1 + \phi_2 + \phi_3 \quad \text{and} \quad \Sigma\psi = \psi_1 + \psi_2 + \psi_3. \tag{28}$$

Substituting eqn (27) into eqn (24), and the result into eqn (23) gives

$$\alpha = 3 \times 180^\circ - \frac{\Sigma\phi + \Sigma\psi}{2} = \text{constant}, \tag{29}$$

i.e., the angle of embrace of a Type I GAE is a constant.

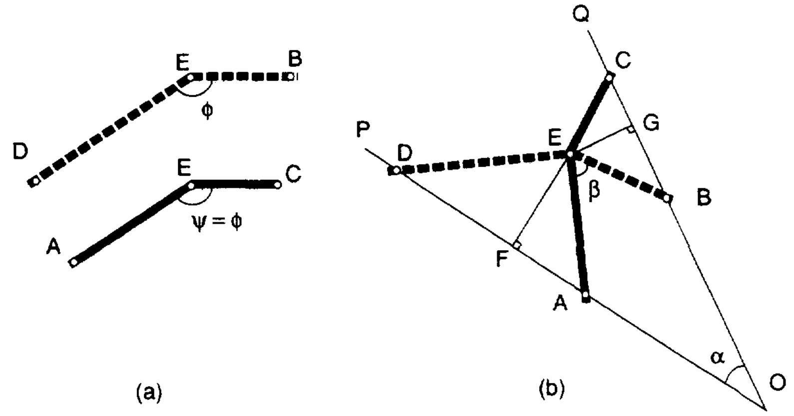

Fig. 6. Simplest Type II GAE, formed by angulated rods with proportional semi-lengths and equal kink angles $\overline{AE}/\overline{DE} = \overline{CE}/\overline{BE}$, $\psi = \varphi$. ADE and BCE are similar triangles.

3.2. *Type II GAE*

Consider first the angulated element shown in Fig. 6, which has

$$\frac{\overline{AE}}{\overline{DE}} = \frac{\overline{CE}}{\overline{BE}}, \quad \text{and} \quad \psi = \phi. \tag{30}$$

To show that the angle α is constant in this case, we note that eqn (14) is still valid. Because $\triangle$AED and $\triangle$BEC are similar,

$$\angle \mathrm{BEG} = \angle \mathrm{DEF} \tag{31}$$

and, substituting eqn (31) into eqn (14)

$$\alpha = 180^\circ - \phi. \tag{32}$$

Note that Hoberman's element is re-obtained when

$$\frac{\overline{AE}}{\overline{DE}} = \frac{\overline{CE}}{\overline{BE}} = 1. \tag{33}$$

A more general Type II GAE is shown in Fig. 7. This element satisfies the following conditions

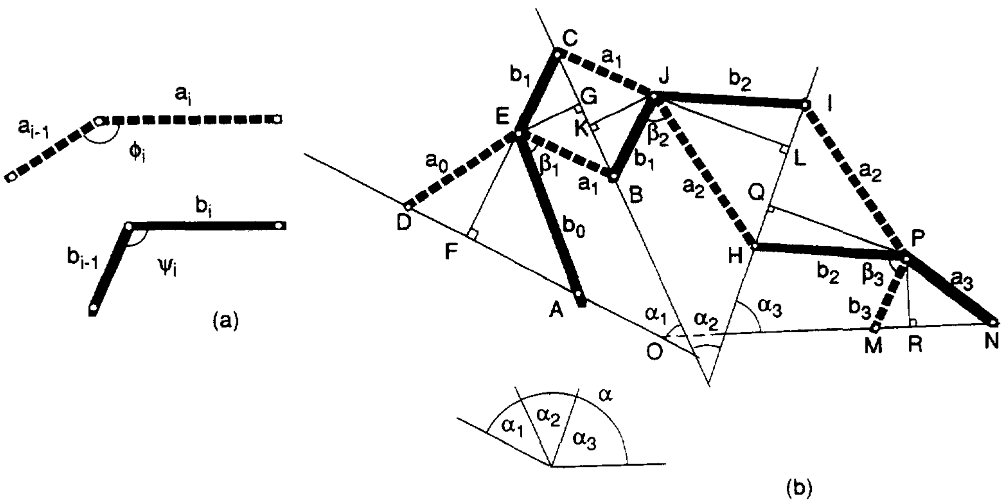

Fig. 7. General Type II GAE consisting of two similar triangles connected by two parallelograms.

(i) each closed loop is a parallelogram
(ii) the triangles on the sides, $\triangle$AED and $\triangle$NPM, are similar, i.e.,

$$\frac{\overline{DE}}{\overline{PM}} = \frac{\overline{AE}}{\overline{NP}} \quad \text{and} \quad \angle AED = \angle MPN. \tag{34}$$

To show that the angle α is constant, we note that eqn (23) is also valid for Type II elements. Also, because of condition (ii)

$$\angle AEF = \angle NPR \tag{35}$$

and, hence, eqn (23) is equivalent to

$$\alpha = 3 \times 180^\circ - \Sigma\psi = \text{constant}. \tag{36}$$

It is interesting to notice that, since

$$\angle AED = \phi_1 - \beta_1 \quad \text{and} \quad \angle MPN = \psi_3 - \beta_3 \tag{37}$$

and since these angles are equal, eqn (25)—also valid for Type II elements—is equivalent to

$$\Sigma\psi = \Sigma\phi \tag{38}$$

which shows that the sum of the kink angles of the two sets of angulated rods that make up a Type II GAE is constant. For angulated elements consisting of two angulated rods only, eqn (38) becomes $\psi = \phi$, which agrees with eqn (30).

3.3. *An additional property of symmetric GAEs*

The use of foldable elements that embrace a constant angle does not guarantee that a structure made from several elements of this type is (i) foldable, and (ii) maintains its shape during folding. Problems can arise due to a radial shift building up within a GAE, and causing the hinges on one side to move by different amounts to the hinges on the other side. It is also possible for a tangential shift to build up, if the hinges on one side of the element move to a line parallel to the original line. Such problems are particularly critical when designing foldable structures that form *closed loops*.

The easiest way round these difficulties is to use symmetric elements. The motion of a GAE with a single, central axis of symmetry is also symmetric, and hence there will be no radial mismatch between hinges on either side.

If only the angulated elements of Section 2 are considered, i.e., those made from two identical angulated rods, then symmetric configurations are obtained only for elements with

$$\overline{AE} = \overline{DE} = \overline{BE} = \overline{CE} \quad \text{and} \quad \psi = \phi. \tag{39}$$

If, however, symmetric GAEs are considered, then many different layouts can be obtained. Some examples are given in Section 5.

4. FOLDABLE CIRCULAR STRUCTURES

Figure 8 shows an assembly of eight identical, symmetric, simple angulated elements, each embracing an angle

$$\alpha = \frac{360^\circ}{8} = 45^\circ. \tag{40}$$

These elements form a closed, circular ring structure whose shape can vary continuously between the shapes shown in Fig. 8(a) and Fig. 8(c), through intermediate shapes as shown in Fig. 8(b). In Fig. 8(a) the deployment angle, defined in Section 2, is $\theta = 45^\circ$ and one set

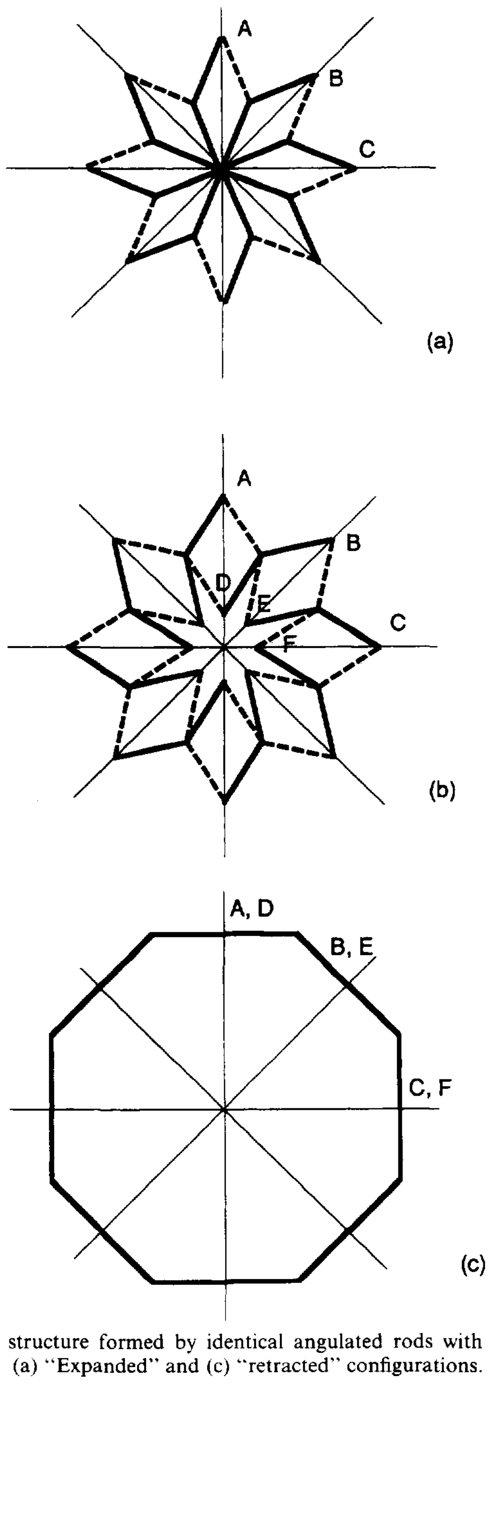

Fig. 8. Foldable ring structure formed by identical angulated rods with a kink angle of 135°. (a) "Expanded" and (c) "retracted" configurations.

of angulated rods (broken lines) is partly hidden by the other set. In Fig. 8(c) the deployment angle is $\theta = 180^\circ$ and one set of rods is completely hidden by the other set.

The hinges of this structure lie on three concentric circles at all times. Note that in Fig. 8(a) one of these circles has shrunk to a point, while in Fig. 8(c) two circles coincide. It is interesting to note that, after reaching a maximum diameter, the circle containing the hinges A, B, C starts to contract, while the other two circles continue to expand. If the physical size of members and joints is neglected, the expansion process terminates when the hinges D, E, and F become coincident with A, B, and C, respectively.

The foldable structure of Fig. 8 is formed by a closed loop of eight *identical rhombuses* and it will be shown in Section 5.1 that in such loops there is no geometric mismatch in different configurations.

The number of angulated elements used in forming a circular loop, as well as the semi-length of the angulated rods, can be varied, but no other changes are possible: all two-dimensional foldable structures with hinges lying on concentric circles are fundamentally of the same type as the structure shown in Fig. 8. This is because each angulated element must be symmetric, and geometric compatibility between adjacent elements requires that all elements remain identical at all stages of folding.

Larger foldable structures based on the solution described above can be formed by inter-connecting two or more concentric circular rings of matching size (Hoberman, 1991). Figure 9 shows the simplest way of doing this, using two *identical ring structures* connected by a series of hinges lying on the circle that contains the hinge A_2. The expansion of this structure is limited by the inner ring becoming fully closed, Fig. 9(a), while its retraction is limited by the outer ring becoming fully stretched. Actually, this is a rather unusual foldable structure. During folding, its outer diameter initially decreases and then increases back to the original value, only the size of the central hole increases monotonically. Actually, this type of behaviour is perfectly suited for large foldable domes, because it is easier to arrange its supports if the perimeter remains approximately constant. The above solution is the key to the Iris Retractable Roof (Hoberman, 1991).

Better packaging of the two concentric rings can be achieved by using a slightly smaller structure for the inner ring. Let $L = \overline{A_2A_3} = \overline{A_3A_4}$ be the semi-length of the angulated elements that make up the outer ring. The optimal value of the semi-length l of the elements of the inner ring, $l = \overline{A_0A_1} = \overline{A_1A_2}$, is such that in the fully-expanded configuration A_0A_2 becomes orthogonal to OP_0. This requires

$$\frac{l}{L} = \cos\frac{\alpha}{2} \tag{41}$$

which, for octagonal rings ($\alpha = 45^\circ$), gives

$$\frac{l}{L} = 0.92.$$

Other values of the ratio l/L are also acceptable, but produce smaller expansion ratios.

Next, it will be shown that *in circular foldable structures made from identical, symmetric angulated elements, contiguous angulated rods can be connected rigidily to one another, to form multi-angulated rods.* Consider two identical angulated rods of semi-length l, lying in neighbouring sectors subtending equal angles α, as shown in Fig. 10. Let node A_2 be the connection point of the two elements. It will be shown that the angle between the two rods, $\angle A_1A_2A_3$, has constant magnitude. Considering the first angulated rod, which lies between the lines OP_0 and OP_2, the distance of hinge A_2 from point O is

$$\overline{OA_2} = \frac{\overline{A_2C_1}}{\sin\alpha/2} = \frac{l\cos(\angle A_1A_2C_1)}{\sin\alpha/2} \tag{42}$$

where

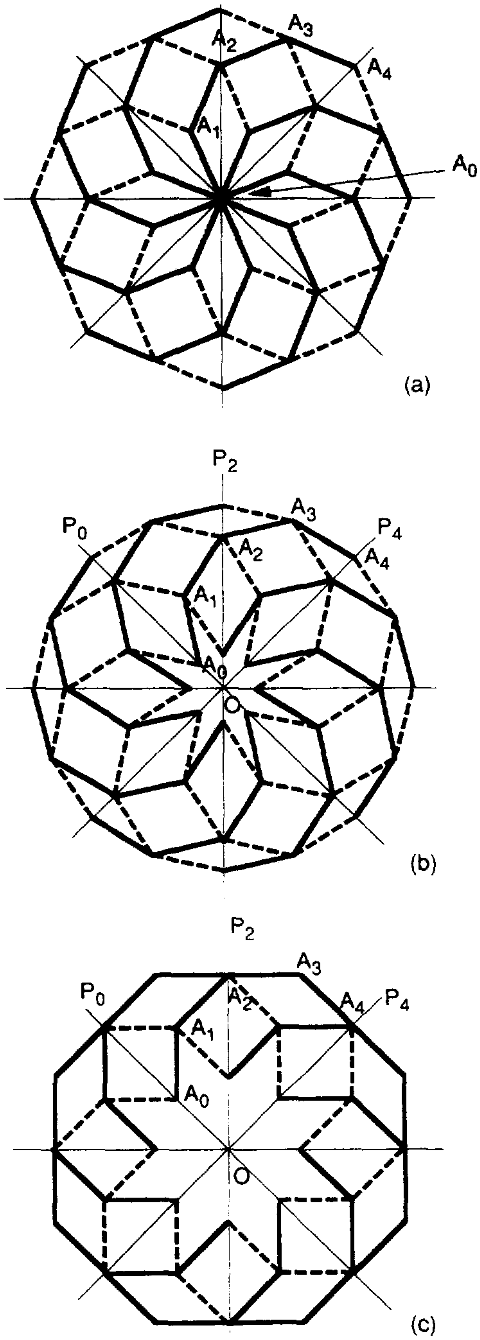

Fig. 9. Foldable circular structure obtained by connecting together two rings like those in Fig. 8. The members $A_0A_1A_2A_3A_4$, etc. are multi-angulated rods.

$$\angle A_1A_2C_1 = 90^\circ - \angle A_2A_1C_1 = 90^\circ - (180^\circ - \angle A_2A_1O). \tag{43}$$

Because

$$\angle A_2A_1O = \angle S_1A_1O + \angle A_2A_1S_1 = \angle S_1A_1O + \frac{180^\circ - \alpha}{2}. \tag{44}$$

Equation (43) becomes

$$\angle A_1A_2C_1 = \angle S_1A_1O - \alpha/2. \tag{45}$$

Substituting eqn (45) into eqn (42)

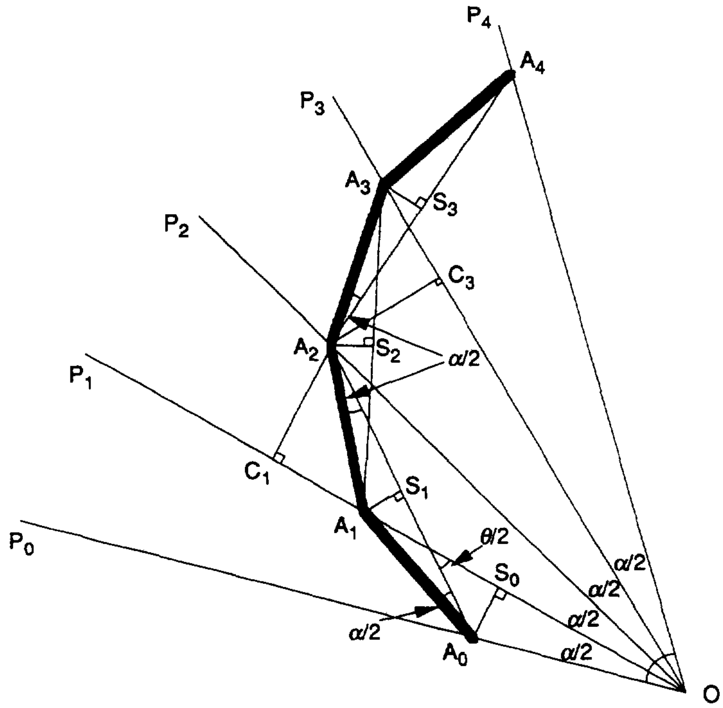

Fig. 10. Multi-angulated rod.

$$\overline{OA_2} = \frac{l\cos(\angle S_1A_1O - \alpha/2)}{\sin\alpha/2}. \tag{46}$$

Also

$$\angle A_1A_2O = 180^\circ - \frac{\alpha}{2} - \angle A_2A_1O = 90^\circ - \angle S_1A_1O. \tag{47}$$

Considering the second angulated rod, the distance of hinge A_2 from point O is

$$\overline{OA_2} = \frac{\overline{A_2C_3}}{\sin\alpha/2} = \frac{l\cos(\angle A_3A_2C_3)}{\sin\alpha/2} \tag{48}$$

where

$$\angle A_3A_2C_3 = \angle S_3A_2C_3 + \alpha/2 = \angle S_3A_3O + \alpha/2. \tag{49}$$

Hence

$$\overline{OA_2} = \frac{l\cos(\angle S_3A_3O + \alpha/2)}{\sin\alpha/2}. \tag{50}$$

Comparing eqn (46) with eqn (50),

$$\angle S_1A_1O - \alpha/2 = \angle S_3A_3O + \alpha/2. \tag{51}$$

Also

$$\angle A_3A_2O = \angle A_3A_2C_3 + 90^\circ - \alpha/2 = 90^\circ + \angle S_3A_3O. \tag{52}$$

The angle between the two angulated elements can be calculated from eqn (47) and eqns (51)–(52).

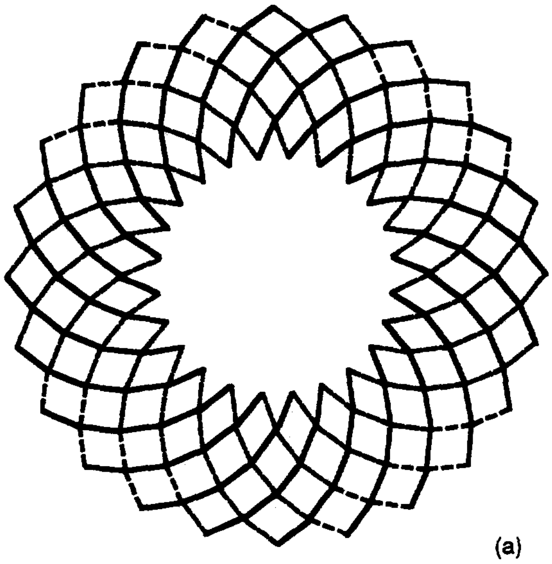

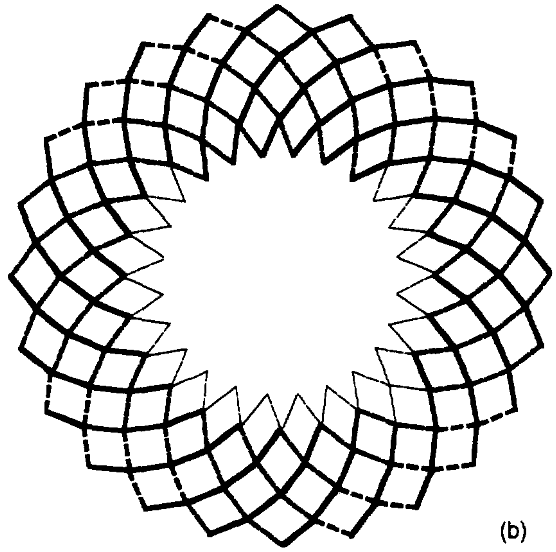

Fig. 11. Foldable circular structures formed by multi-angulated rods with kink angles of 165°.

$$\angle A_1A_2A_3 = \angle A_1A_2O + \angle A_3A_2O$$
$$= 180° + \angle S_3A_3O - \angle S_1A_1O = 180° - \alpha = \text{constant.} \quad (53)$$

This proof can be extended to any number of contiguous rods of equal semi-length l, provided that they are at a non-decreasing distance from the centre: when they start to turn back towards the centre, the angle $\angle S_iA_iO$ becomes negative and hence the above proof is no longer valid. Subject to this condition, the rods can be rigidly linked together to form a multi-angulated rod with a kink angle of $180° - \alpha$, eqn 53.

Figure 11(a) shows a circular foldable structure containing 48 five-segment multi-angulated rods. This structure has

$$\alpha = \frac{360}{48/2} = 15°.$$

Figure 11(b) shows that modest shape changes can be made by varying the number of segments in some rods. Figure 12 shows photographs of a model structure with

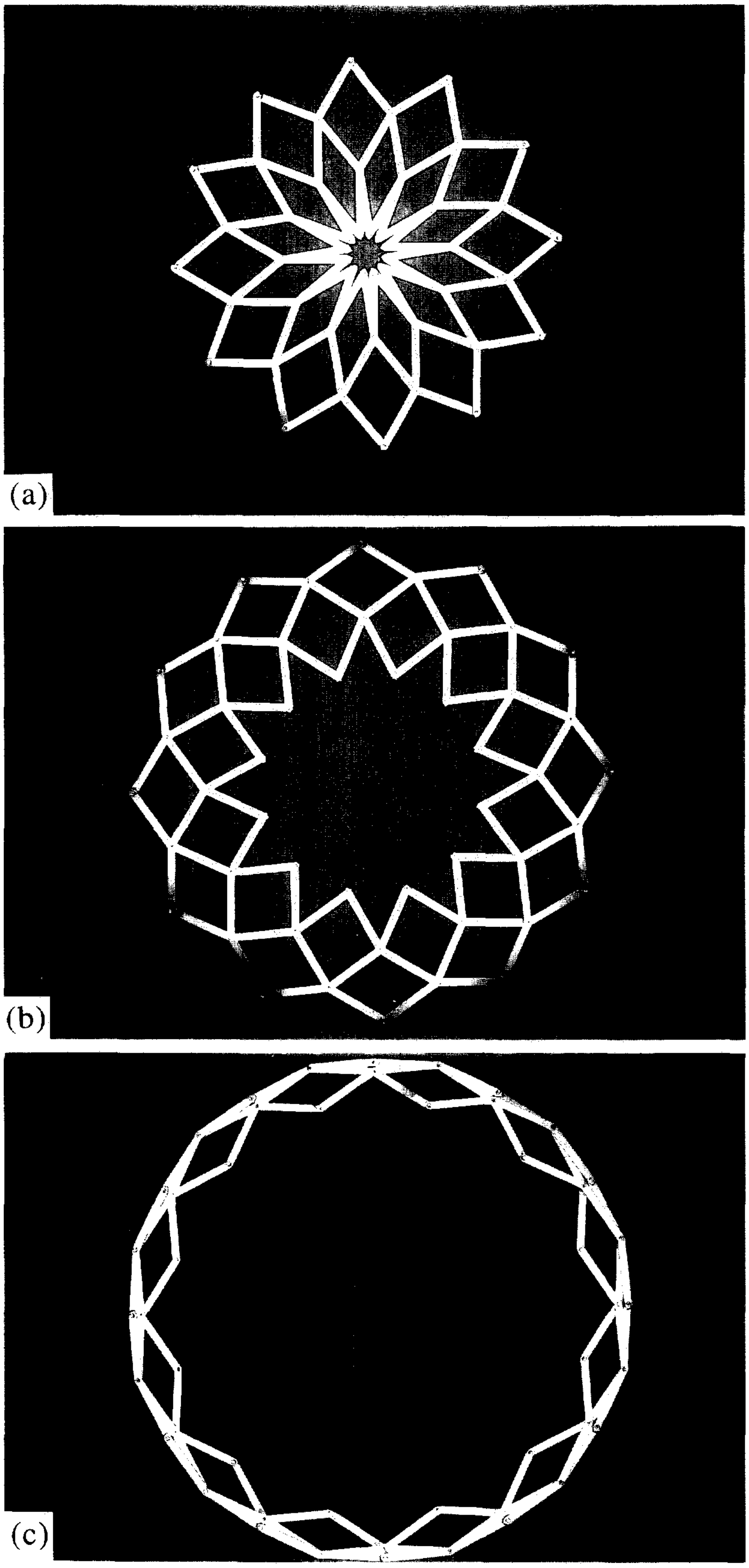

Fig. 12. Model structure built from 24 identical three-segment, multi-angulated rods.

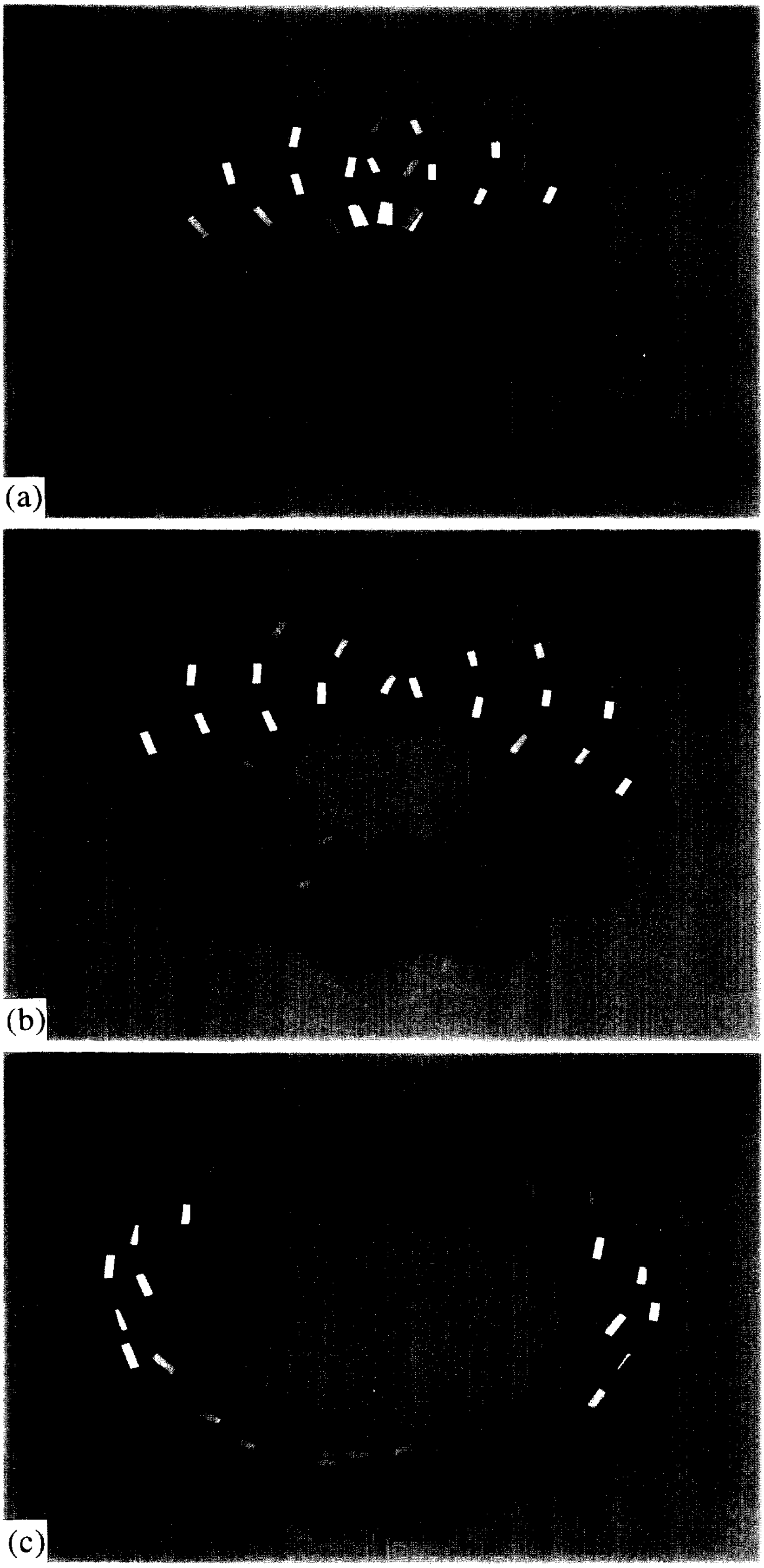

Fig. 19. Double-layer circular foldable structure with curved upper layer.

$$\alpha = \frac{360}{24/2} = 30^\circ$$

whose 24 identical multi-angulated rods have kink angles of 30°, and each rod consists of three segments of length $l = 100$ mm. The fully-deployed and fully-folded configurations of this model are shown in Fig. 12(a) and Fig. 12(c), respectively. Note that the rods cannot fully overlap because of the physical size of the joints.

5. FOLDABLE STRUCTURES OF GENERAL SHAPE

It might be expected that two-dimensional foldable structures with many different shapes might be made by a straightforward extension of the ideas introduced above. Indeed, an obvious way of doing this would be to divide any given boundary shape into straight segments and circular arcs, and then assemble together straight-edged, trellis-type structures of suitable length, Fig. 1, and simple angulated elements with an appropriate angle of embrace. Unfortunately, a bar structure of this type is not foldable. The problem is that, although it is possible to vary the semi-length of the simple angulated elements that make up a circular sector, so that the hinges connecting this sector to its neighbouring trellis-type structure are equally, or proportionally spaced in the radial direction, this can be done only for *a particular configuration*. The scissor hinges do not remain equally spaced when the configuration is varied. Hence, a circular sector cannot be connected to a structure consisting of straight rods, whose scissor hinges are always equally, or proportionally spaced.

To obtain the layout of a two-dimensional foldable structure with a boundary of prescribed shape one must begin by finding a *foldable base structure*, i.e., a structure consisting of angulated rods whose hinges lie on the prescribed boundary. Once a suitable layout for the base structure has been selected, extra members can be connected to it by means of scissor hinges, until the required shape and overall dimensions are obtained. It will be shown that such a structure is foldable and, subject to certain conditions, it remains foldable if contiguous bars are firmly connected, thus forming a series of multi-angulated rods.

5.1. *Layout of the base structure*

Finding a base structure that meets all the shape and folding requirements of a given application is the key to a successful overall solution and yet there is no unique set of rules leading automatically to the best layout of angulated elements. Therefore, the method will be explained by describing the procedure which has been followed for a series of representative examples. All of the examples are of the same basic type, continuous loop structures with a central hole of variable size. Such structures are suitable for foldable roofs for, e.g. sports stadia and tennis courts. Open loop structures are subject to fewer restrictions, and hence much easier to configure using any combination of GAE's.

Figure 13 illustrates a simple technique (Hoberman, 1990) to construct a single-loop foldable bar structure of any shape. Figure 13(a) shows an illustrative, general polygon which may be constructed from a series of Hoberman's elements whose internal hinges coincide with the vertices of the polygon. The semi-length of each angulated rod is equal to half the length of each side and the two rods belonging to the same element form equal kink angles, which are equal to the internal angle of the polygon. Hence, in the fully folded configuration, Fig. 13(b), the elements overlap with the sides of the polygon. Note that half of the angulated rods are hidden by the other rods. In general, of course, these angulated elements are not symmetric and hence, according to Section 3.3, a radial mismatch develops as the structure is folded. However, the overall mismatch adds up to zero, Fig. 13(c), because in this case the angulated elements form a chain of *similar rhombuses* whose diagonals are reduced in length by proportional amounts and also remain at constant angles during folding.

Figure 14 shows a more general type of closed loop structure, whose internal hinges also coincide with the vertices of the polygon of Fig. 13(a). Here, the angulated rods making

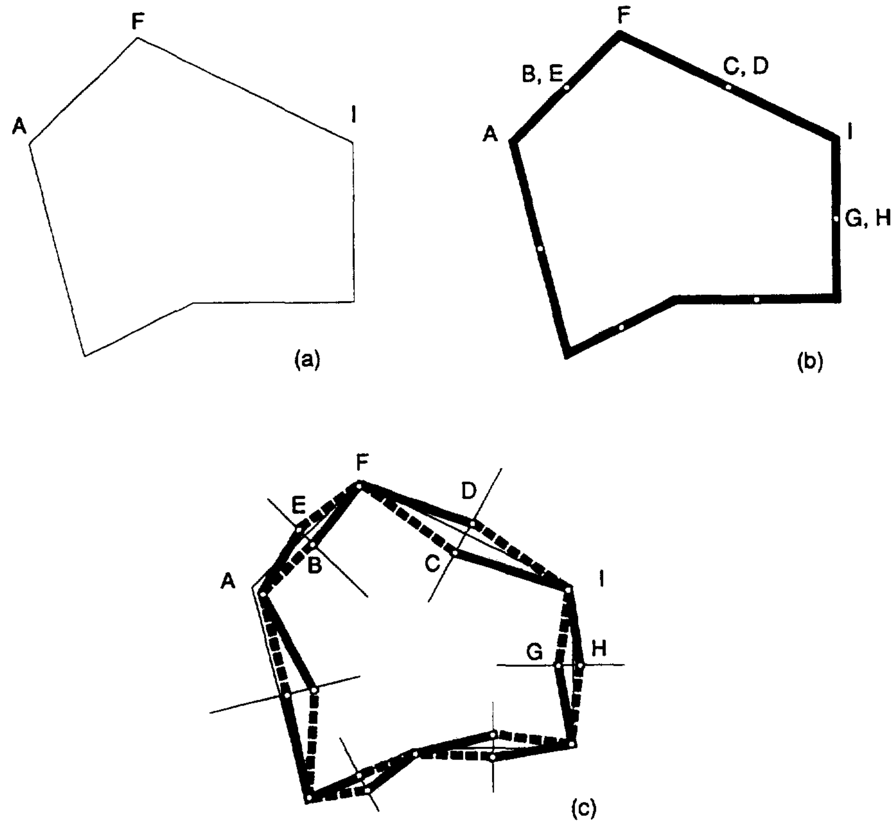

Fig. 13. Foldable closed loop structure which folds along a given polygon. The angulated elements form similar rhombuses.

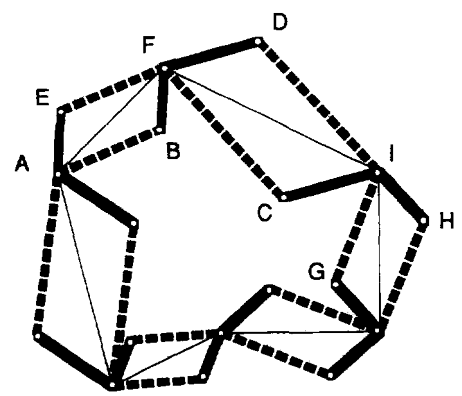

Fig. 14. Foldable closed loop structure which folds along the polygon of Fig. 13, but consists of similar parallelograms.

up each element are no longer identical, but still have a kink angle equal to the internal angle of the polygon, and form a chain of *similar parallelograms*. This property implies that the loop structure is foldable, because the sides of the polygon vary by proportional amounts and hence no geometric mismatch builds up during folding. Note that each of the six angulated elements used in this solution is a Type II GAE without any parallelograms, as that shown in Fig. 6.

In addition to the above solutions for base structures forming closed loops of any shape, greater freedom is available in the case of loops with one or more axes of symmetry. Basically, any GAE can be used to form the basic repeating unit and since, by symmetry, all units behave in the same way, geometric compatibility in all configurations is automatically

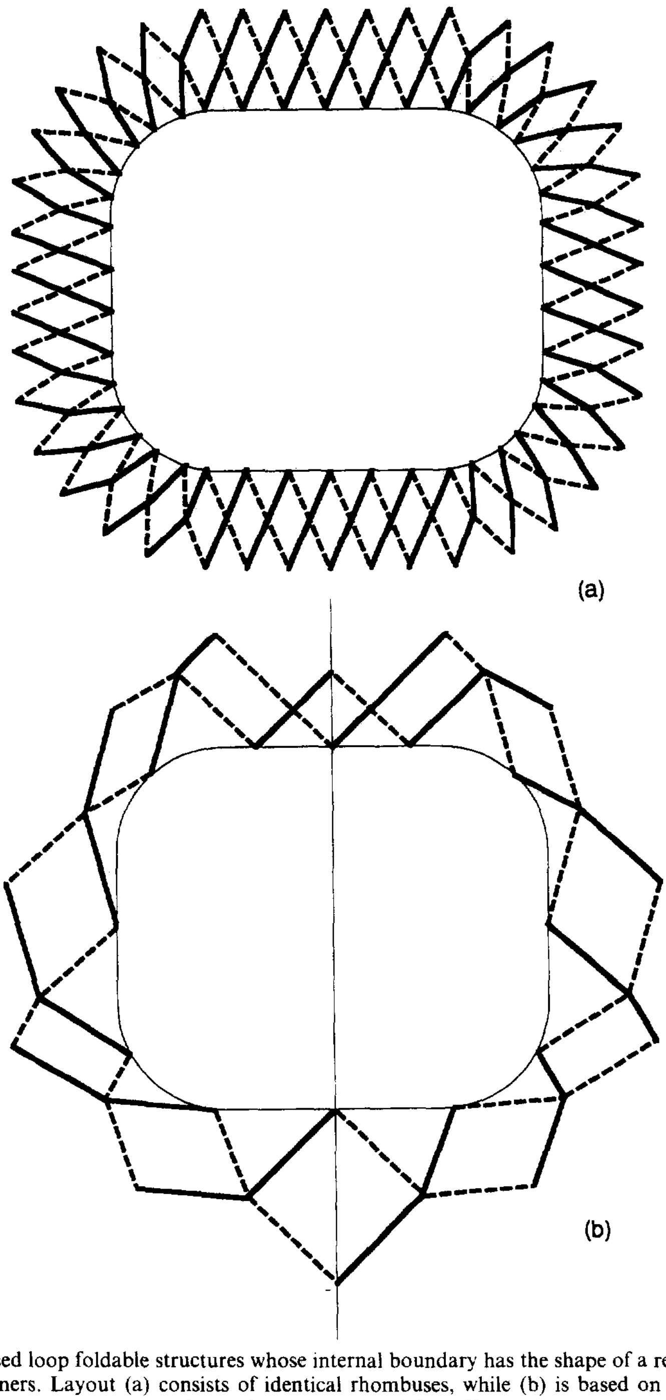

Fig. 15. Closed loop foldable structures whose internal boundary has the shape of a rectangle with rounded corners. Layout (a) consists of identical rhombuses, while (b) is based on a symmetric GAE of both Type I and Type II.

satisfied. Figure 15 shows two loop structures whose innermost hinges lie on a rectangle with rounded corners. The base structure shown in Fig. 15(a) consists of identical rhombuses, and hence there is no need to invoke symmetry to prove that this structure is foldable. The base structure shown in Fig. 15(b), though, is based on a symmetric arrangement of GAEs which are both of Type I and Type II. This can be seen by means of the central line of symmetry that has been drawn in Fig. 15(b), which divides two opposite rhombuses into pairs of similar isosceles triangles.

5.2. *How to extend the base structure*

Any base structure can be extended by the addition of a pair of bars of any length, connected to one another and to the base structure by scissor hinges. The resulting structure

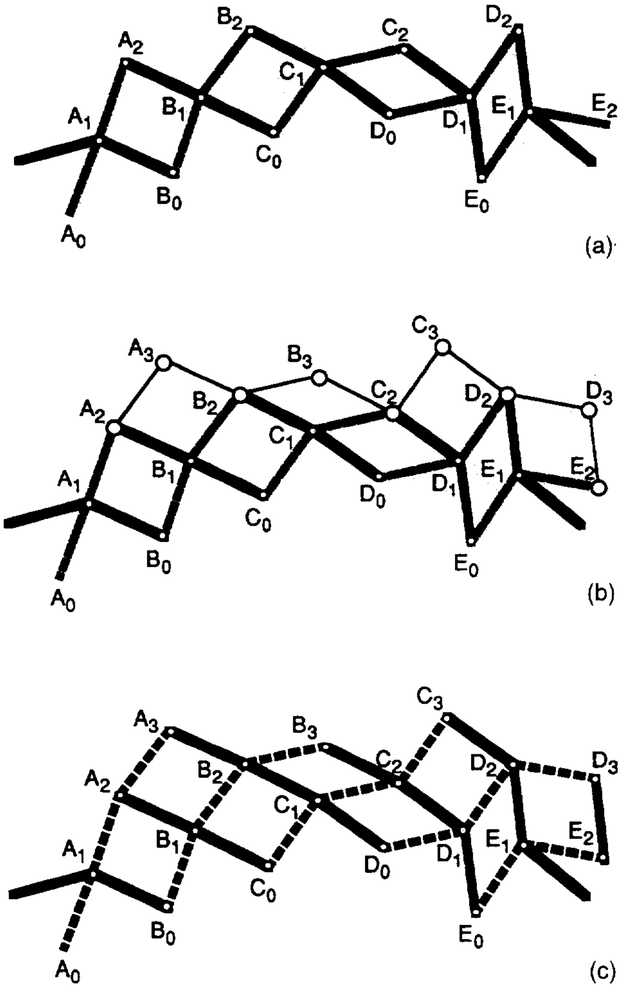

Fig. 16. Three foldable structures: (a) base structure consisting of several parallelograms; (b) extended structure, with additional hinged bars; (c) rigidly-connected structure formed by multi-angulated rods.

will be foldable, like the original base structure, provided that the members added to it are not collinear. Repeating the same argument it can be shown that any number of pairs of bars connected by hinges to the base structure will leave its mobility unchanged.

Of greatest practical importance is the particular case of a base structure consisting of a series of parallelograms, as in Figs 13–15.

Figure 16(a) shows a general, small part of a bar structure consisting of angulated elements. Additional members are connected to its outer hinges, Fig. 16(b), such that the quadrangles $A_2A_3B_1B_2$, etc. are *parallelograms*. This extended structure is foldable because all additional members are free to rotate with respect to the base structure but, in fact, no relative rotation between consecutive rods occurs as the structure is folded. i.e., $\angle A_1A_2A_3$, $\angle B_1B_2B_3$, etc. remain constant. Consider, for example, $\angle A_1A_2A_3$. Because A_1A_2 and A_2A_3 remain parallel to B_0B_1 and B_1B_2, respectively,

$$\angle A_1A_2A_3 = \angle B_0B_1B_2 = \text{constant} \tag{54}$$

since $\angle B_0B_1B_2$ is the kink angle of an angulated rod, which is fixed.

In conclusion, this foldable structure can be made from multi-angulated rods similar to those introduced in Section 4, as shown in Fig. 16(c), but note that the kink angles along these rods are no longer equal. The same procedure is valid for all other closed loop base

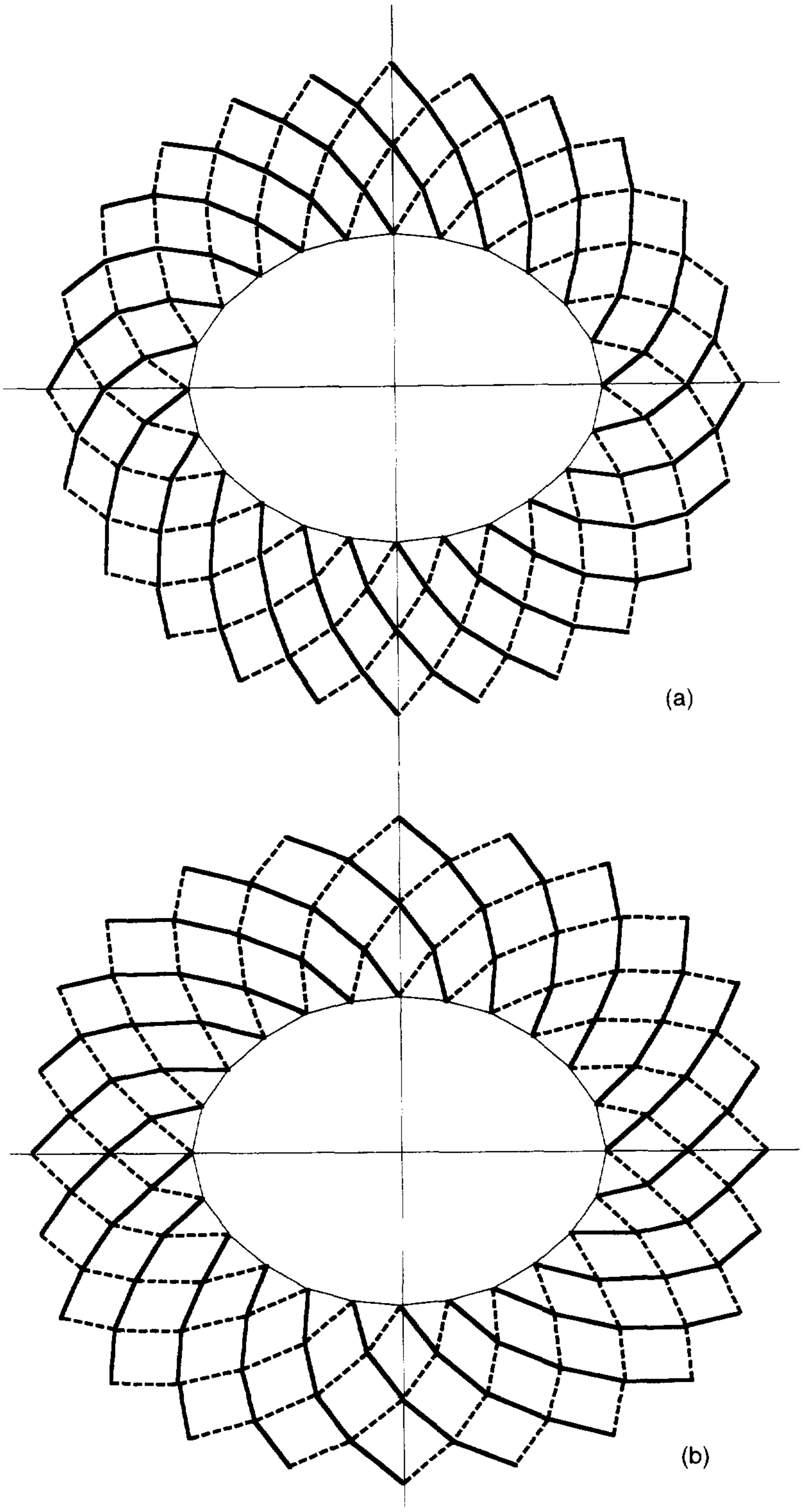

Fig. 17. Foldable elliptical structures formed by multi-angulated rods forming tessellations of (a) rhombuses and (b) parallelograms.

structures discussed in this section, as for any open loop base structure. Figure 17 shows two symmetric foldable structures whose internal boundaries have an identical elliptical shape. In both structures, the inner joints are equally spaced but, while the first layout is a tessellation of rhombuses whose side lengths are all equal, the layout of Fig. 17(b) is a tessellation of parallelograms, whose side lengths are not all equal.

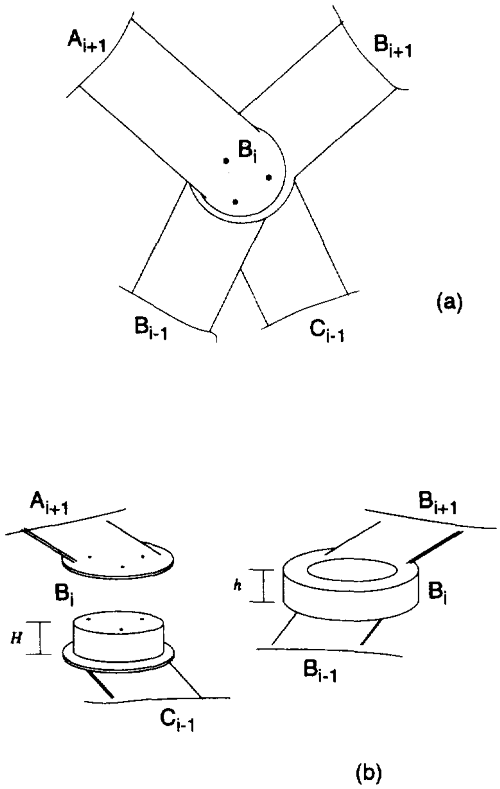

Fig. 18. Detail of joint of dome structure.

6. DOME STRUCTURES

The two-dimensional solutions derived above easily extend to curved structures, by projecting any two-dimensional solution onto a surface with the required shape. Thus, each multi-angulated rod can be curved out of plane. Of course, all connectors between multi-angulated rods should be perpendicular to the plane of projection.

The folding angle may be restricted if the rods are not allowed to overlap during folding. This problem can be solved by a proper design of the connections. An example of a suitable connector between two rods is shown in Fig. 18. In the drawings, B_{i-1} B_i B_{i+1} is one of the rods, whilst the other rod A_{i+1} B_i C_{i-1} is in two parts. B_i C_{i-1} has a circular cross-section cylindrical post of height H and A_{i+1} B_i has a cap which can be fitted onto the post. B_{i-1} B_i B_{i+1} is fitted with an open ring at B_i of height $h < H$, so that a relative rotation of the two rods can take place.

Figure 19 shows a double layer model structure whose curved top layer is connected to the flat bottom layer by long bolts. The bottom layer is identical to the model shown in Fig. 12, and the orthogonal projection of the top layer onto the plane of the bottom layer is also identical to it. This model folds until the outer rods overlap fully, and thus demonstrates that the interference between rods connected to the same hinge has been successfully eliminated. Note that bracing elements could be added between the upper and lower cords, to increase the stiffness of the structure, if desired.

7. DISCUSSION AND CONCLUSIONS

A general method for the design of two-dimensional foldable structures has been introduced. The new method extends and generalises the trellis-type structures, based on a tiling of parallelograms whose sides are collinear, to structures based on any tiling of parallelograms. It has been shown that a bar structure of this type is (i) foldable and (ii) can be made from multi-angulated, rigid rods connected by scissor hinges. This result affords much greater freedom in the range of shapes that can be achieved, and of boundary conditions that can be met. This approach can be easily extended to three-dimensional dome structures.

Also, a family of elements for foldable structures has been introduced. These elements consist of angulated rods connected by scissor hinges. It has been shown that any element bounded by either isosceles triangles or similar triangles, with any number of parallelograms in between, maintains a constant angle of embrace.

Finally, a method for the design of structures consisting of multi-angulated rods that fold along their perimeter has been introduced, and there is practically no limit to the range of perimeter shapes that can be achieved.

These new solutions have significant implications for the design of foldable structures. Because continuous members are used throughout, the complexity of the joint is reduced and more efficient structural design become possible, e.g., curved trusses can be used instead of beams. Also, the attachment of covering panels or membranes is simplified.

REFERENCES

Clarke, R. C. (1984) The kinematics of a novel deployable space structure system. In *Proceedings of the Third International Conference on Space Structures*, 11–14 September, 1984, University of Surrey, Guildford, ed. H. Nooshin, pp. 820–822, Elsevier Applied Science Publishers, Barking.

Escrig, F. (1985) Expandable space structures. *International Journal of Space Structures* **1**, 79–91.

Escrig, F., Valcarcel, J. P. and Delgado, O. G. (1989) Design of expandable spherical grids. In *Proceedings of* 10 *Years of Progress in Shell and Spatial Structures*, 30 *Anniversary of IASS*, Madrid, Spain, eds F. d. Pozo and A. d. l. Casas, IASS.

Escrig, F. (1993) Las estructuras de Emilio Perez Pinero. In *Arquitectura Transformable*, pp. 11–32, Escuela Tecnica Superior de Arquitectura de Sevilla.

Escrig, F. and Valcarcel, J. P. (1993) Geometry of expandable space structures. *International Journal of Space Structures* **8**, 71–84.

Gantes, C., Connor, J. J. and Logcher, R. D. (1991) Combining numerical analysis and engineering judgement to design deployable structures. *Computers and Structures* **40**, 431–440.

Hoberman, C. (1990) Reversibly expandable doubly-curved truss structure. *US Patent* 4,942,700.

Hoberman, C. (1991) Radial expansion/retraction truss structures. *US Patent* 5,024,031.

Kwan, A. S. K. and Pellegrino, S. (1991) The pantographic deployable mast: design, structural performance and deployment tests. In *Rapidly Assembled Structures*, ed. P. S. Bulson, pp. 213–224, Computational Mechanics Publications, Southampton.

Levy, M. P. (1995) Retractable lightweight structures. In *Proceedings of Spatial Structures: Heritage, Present and Future*, 5–9 June, 1995 Milano, ed. G. C. Giuliani, pp. 511–515, SGE Editoriali, Milan.

Pellegrino, S. and You, Z. (1993) Foldable ring structures. In *Space Structures* 4, *Proceedings of the Fourth International Conference on Space Structures*, Guildford, 6–10 September 1993, eds G. A. R. Parke and C. M. Howard, pp. 783–792, Thomas Telford, London.

Pinero, E. P. (1961) *Spain Patent Number* 266801.

Servadio, I. (1994) Deployable regular and semi-regular polyhedral structures using Hoberman's technique. In *Proceedings of Application of Structural Morphology to Architecture: Second Int. Seminar on Structural Morphology*, Stuttgart, 8–9 October, 1994, eds R. Holler, J. Hennicke and F. Klenk, pp. 171–180, IL, University of Stuttgart.

Waters, T. (1992) The unfolding world of Chuck Hoberman. *Discover*, March, pp. 70–78.

You, Z. and Pellegrino, S. (1994) Deployable mesh reflector. In *Spatial, Lattice and Tension Structures, Proceedings of IASS-ASCE Symposium*. Atlanta, April 1994, eds J. F. Abel, J. W. Leonard and C. U. Penalba, pp. 103–112, ASCE, New York.

You, Z. and Pellegrino, S. (1996) Expandable/collapsible structures. *British Patent Application no.* 9601450.1

Zanardo, A. (1986) Two-dimensional articulated systems developable on a single or double curvature. *Meccanica* **21**, 106–111.

Zeigler, T. R. (1981) Collapsible self-supporting structures and panels and hub therefor. *USA Patent no.* 4290244.

Zeigler, T. R. (1984) Collapsible self-supporting structures. *USA Patent no.* 4437275.

Zeigler, T. R. (1987) Portable shelter assemblies. *USA Patent no.* 4689932.

Zeigler, T. R. (1993) Polyhedron building system. *USA Patent no.* 5230196.